Swiss J Palaeontol (2011) 130:7–18
DOI 10.1007/s13358-010-0003-2

Ordovician–Silurian Lilliput crinoids during the end-Ordovician biotic crisis

Matthew R. Borths · William I. Ausich

Received: 28 July 2010 / Accepted: 23 September 2010 / Published online: 2 December 2010

Abstract Coincident with the end-Ordovician (end-Katian for crinoids) biodiversity crash, crinoids from Anticosti Island, Quebec, experienced a statistically significant reduction in body size, an evolutionary trend termed the "Lilliput Effect". This decrease in body size occurred for the fauna as a whole, and data indicate that neither dominant Ordovician nor dominant Silurian clades experienced preferential size decrease. Because the post-extinction fauna with a diminished size is composed of largely new taxa, this example of the Lilliput Effect is regarded as the miniaturization mode. The miniaturization occurred very rapidly; however, the recovery on Anticosti Island did not occur for as many as 7 Ma. This macroevolutionary asymmetry, as demonstrated in many other studies, highlights the need to preserve the biodiversity present on Earth today.

Keywords Crinoids · Ordovician · Silurian · Extinction · Lilliput Effect

Introduction

The end-Ordovician records the second largest biosphere collapse during Earth history (Sepkoski 1981; Brenchley 1989 Brenchley et al. 1994). An estimated 57% of genera and 25% of families went extinct during this interval, dramatically affecting the diversity of major groups. A few examples include graptolites (Chen et al. 2003), brachiopods (Harper and Rong 1995; Sheehan 2001), conodonts (Barnes and Bergström 1988), crinoids (Eckert 1988; Donovan 1989; Donovan 1994) (Peters and Ausich 2008), reef faunas (Copper 2001) and many others (e.g., Hallam and Wignall 1997; Finney et al. 1999; Sheehan 2001; Kaljo et al. 2008; and others).

It is generally thought that the end-Ordovician biotic crisis resulted from global climate change that concluded in a glacial epoch (Brenchley et al. 2003). With the buildup of ice on Gondwana, sea level fell, resulting in a catastrophic loss of marine habitats (e.g., Berry and Boucot 1973; McKerrow 1979; Sheehan 2001). Many hypotheses have been advanced to explain the global changes at this time, including nutrient levels in the ocean, uplift on the continents, rates of silicate and carbonate weathering, reduction of poleward heat transfer in the oceans, orbital eccentricity cycles, gamma ray bursts, volcanic eruptions, among others (e.g., Kump et al. 1999; Sutcliffe et al. 2000; Sheehan 2001; Herrmann et al. 2004a; Melott and Thomas 2009; Young et al. 2010). Originally thought to be relatively short (Brenchley et al. 1994), this glacial epoch is now recognized to have continued through the Llandovery (Grahn and Caputo 1992; Grahn and Caputo 1994; Brenchley et al. 2003; Ghienne 2003; Herrmann et al. 2004b; Lefebvre et al. 2010). Widespread, epicontinental seas returned during the middle to late Telychian and into the Wenlock.

As a result of the fall in sea level, a significant Ordovician–Silurian unconformity exists in most parts of the world, which has made it difficult to characterize the biotic collapse and recovery during this interval. Anticosti Island, Quebec, is a noteworthy exception because a shelly fossil record occurs across the Ordovician–Silurian

M. R. Borths (✉)
Department of Anatomical Sciences, Stony Brook University, Stony Brook, NY 11794, USA
e-mail: Matthew.Borths@stonybrook.edu

W. I. Ausich
School of Earth Sciences, The Ohio State University, 155 South Oval Mall, Columbus, OH 43210, USA
e-mail: ausich.1@osu.edu

boundary in a nearly complete section from the upper Katian through much of the Telychian (Fig. 1). We utilize this boundary section to explore the changing morphology of crinoids through the Ordovician–Silurian biodiversity crisis.

Paleozoic crinoids are divided into three macroevolutionary faunas: early Paleozoic crinoid evolutionary fauna (CEF), middle Paleozoic CEF, and late Paleozoic CEF. These evolutionary faunas are distinct at high taxonomic levels, i.e., subclasses and orders (Baumiller 1993; Ausich et al. 1994). The end-Ordovician biotic crisis was significant for crinoid evolutionary history; it coincided with the change from the early Paleozoic to the middle Paleozoic CEF. The early Paleozoic CEF fauna was dominated by disparid, diplobathrid camerate, and hybocrinid crinoids and existed throughout the Ordovician. After the end-Ordovician extinction, the middle Paleozoic fauna, characterized by cladid, monobathrid camerate, and flexible crinoids became dominant. End-Ordovician extinctions among crinoids were studied by Eckert (1988). Significant new crinoid faunas have been described recently from Anticosti Island (Ausich and Copper 2010), and Peters and Ausich (2008) combined these new data with a revised, global compendium of Ordovician through Llandovery crinoid faunas. At a global scale, an end-Ordovician crinoid mass extinction was confirmed (Peters and Ausich 2008). A single significant extinction event occurred at the end of the Katian, and crinoid faunas did not fully assume the characteristics of a typical middle Paleozoic fauna until the late Llandovery. A pattern observed during collection of the Anticosti Island specimens was that crinoids from formations immediately above and below the Ordovician–Silurian boundary were generally smaller than specimens either stratigraphically higher or lower than the boundary interval. If so, this would be a Paleozoic example of the "Lilliput Effect" (Urbanek 1993; Twitchett 2006; Harries and Knor 2009 and references cited therein). The present study tests this field observation to determine whether the end-Ordovician biotic crisis was associated with body-size reduction of crinoids on Anticosti Island. Furthermore, if present, how was this change manifest within crinoid clades, as well as the entire fauna?

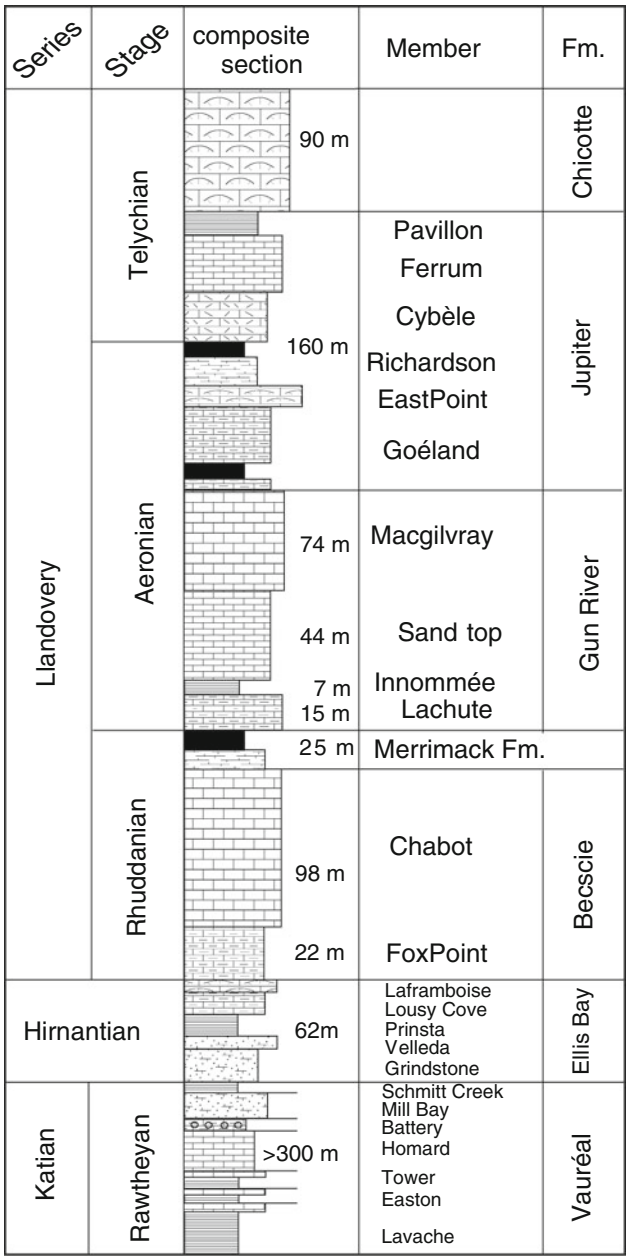

Fig. 1 Stratigraphic section on Anticosti Island from Jin and Copper

Lilliput Effect

Size is among the most recognizable attribute of an organism. Therefore, it is not surprising that evolutionary trends in body size changes have been recognized for some time and now codified as "Cope's Rule" and "Lilliput Effect" (for example, see Stanley 1973; Hone and Benton 2005; Hone et al. 2005; Hone and Benton 2007). Urbanek (1993) coined Lilliput Effect for a trend of size reduction and rebound in a Late Silurian graptolite fauna. During a relatively minor episode of Late Silurian paleoenvironmental change, graptolite species became smaller; and after the environment returned to favorable conditions, the average body sizes of the affected taxa rebounded to pre-event dimensions.

The Lilliput Effect is now used to describe a general ecologic or evolutionary trend in the reduction of body size (Harries and Knor 2009). This general phenomenon is now recognized among many taxonomic groups through extinction episodes of various magnitudes, especially the

big five extinction intervals. Examples, among many, include Early Silurian corals (Kaljo 1996), Late Silurian graptolites (Urbanek 1993), Late Devonian conodonts (Girard and Renaud 1996), Late Permian gastropods and bivalves (Twitchett 2007), Late Permian brachiopods (Weihong et al. 2006), Cenozoic foraminifera (Schmidt et al. 2004; Wade and Olsson 2009), and Cenozoic bivalves (Lockwood 2005).

In the current broader definition of the Lilliput Effect, the evolutionary trend toward small body size may occur in four ways. (1) The body size of individuals within a species may decrease during a biotic crisis and recover thereafter, which is the original Urbanek (1993) concept. Harries and Knor (2009) referred to this as "dwarfing," and Twitchett (2006) termed this "within-lineage size decrease". (2) "Faunal stunting" (Harries and Knor 2009) occurs when the surviving taxa are preferentially smaller. This is a form of species sorting and was referred to as the "extinction of large taxa" mode of Twitchett (2006). (3) "Miniaturization" is the origination of taxa after the extinction with smaller-sized species than present in predecessor lineages. (4) A pattern of decrease in average body size after an extinction could result from large taxa with post-extinction Lazarus gaps (Twitchett 2006).

The patterns of size change through time are easier to detect than the identification of a single or multiple cause(s) driving this evolutionary trend. A series of potential causes have been suggested by several authors, including biotic collapse in primary productivity, change in salinity, change in oxygen levels, general biotic stress, temperature change, and loss of symbiotic associates (Lockwood 2005; Wade and Peterson 2008; Wade and Twitchett 2009). Harries and Knor (2009) also suggested the "Island Rule" (Van Valen 1973) and "Bergmann's Rule" (Bergmann 1847; Meire and Dayan 2003). The Island Rule posits that larger organisms tend to become smaller when they invade an island with limited resources. Bergmann's Rule involves geographic/latitudinal replacements. The latter has been proposed for Ordovician–Silurian faunas (Rong et al. 2006) and Frasnian-Famennian faunas (Copper 1986).

Anticosti Island stratigraphy

Anticosti Island is approximately 200 km long and 50 km at its widest point and is situated near the mouth of the St. Lawrence River in Quebec, Canada. More than 850 m of strata are exposed on the island, most of which are from shallow marine, shelly depositional facies (Fig. 1). The Anticosti Island stratigraphic section records nearly continuous mixed carbonate and siliciclastic sedimentation from the upper Katian (later Ordovician) through most of the Llandovery (early Silurian). Thus, the end-Ordovician biodiversity collapse and recovery is preserved here in shelly facies better than anywhere else. Deposition and preservation of the Anticosti succession resulted from a complex history, the last phases of which include deposition in the Anticosti foreland basin and the fact that this region has been largely unaffected by deformation associated with orogenic activity along eastern North America (Waldron et al. 1998; Copper and Long 1998; Long 2007; and others).

Biostratigraphic, chronostratigraphic, and sequence stratigraphic studies continue on strata from the Anticosti Section (e.g., Desrochers et al. 2010). The stratigraphy from Copper and Long (1998) is used here; and it is clear that the Vauréal Formation represents the upper Katian, and all or most of the Ellis Bay Formation is within the Hirnantian. The earliest Llandovery, the Rhuddanian, includes the Becscie and Merrimack Formations. The Aeronian (middle Llandovery) includes the Gun River Formation and the lower Jupiter Formation (Goéland through Richardson members). The youngest portion of the Anticosti Island section (Cybéle Member of the Jupiter Formation through the Chicotte Formation) is Telychian (Long and Copper 1987; Copper and Long 1989, 1998; Copper 2001.

Methods

Calyx volume is used as a proxy for crinoid body size. The calyx is a finite morphological element that is relatively commonly preserved. Also, in most instances crinoid species and genera can be identifiable based primarily on calyx morphology. The calyx is defined from the top of the column to the position where the arms become free from the calyx (Ausich et al. 1999, which may be either at the radial plate or following fixed brachials and interradial plates). Two measurements were taken for every known adult Anticosti Island crinoid specimen with sufficient preservation: (1) the maximum calyx height (from the top of the column to the position where arms became free); and (2) the maximum calyx diameter (Ubaghs 1978). Generally, the maximum diameter is at the distal end of the calyx where the arms become free. However, in crinoids with an ellipsoidal calyx shape, the maximum diameter is below the level where arms become free.

In the majority of specimens, calyx shape was classified as either a cone, bowl, or ellipsoid (Ubaghs 1978, fig. 72). Cone-shaped calyxes have straight margins leading from a position near the intersection with the column to the maximum width at the origination of the free arms. Bowl-shaped calyxes have convex calyx sides, yielding nearly a semi-circular cross-section with the maximum width at the origin of the free arms. Ellipsoidal calyxes have a

pseudo-elliptical cross-section with the widest diameter of the calyx below the distal margin of the calyx.

Given the maximum calyx height, maximum calyx diameter, and calyx shape, the overall volume of the calyx was approximated with standard volume calculations for a cone, a hemisphere, and an ellipsoid. Calyx volume could be adequately approximated in this way for all crinoids except the unusual, bilaterally symmetrical Calceocrinidae (see Ubaghs 1978). The volume of the calceocrinid calyx was estimated as a box, so height, width, and depth were measured.

None of the calyxes conformed precisely to any of these ideal geometric forms. However, the idealized shapes do approximate volume for these crinoids, and inaccuracies in volume estimates because of deviation from the ideal shapes are considered insignificant compared to the four orders of magnitude of volume range among Anticosti crinoid calyxes. Calyx dimensions were measured, and volume was estimated for 150 Anticosti Island specimens and 570 specimens were identified to species and used herein. Taxonomic identifications follow Ausich and Copper (2010).

All crinoids complete enough to measure the calyx height and width are included, with the exception of specimens that are clearly juveniles. Juvenile crinoids are recognizable because they have abnormally high and narrow brachials (Brower 1978), in addition to a relatively small size.

In order to portray more accurately the calyx size distribution among Anticosti Island crinoids, all identifiable specimens from each formation were included in the analysis. Data for taxon means and measured specimens only are also given. Mean calyx volumes among formations were compared using the Mann–Whitney *U* test (Hammer et al. 2001).

For bootstrapping, pair-wise comparisons were made of calyx volume between adjacent stratigraphic units (Resampling Stats8 http://www.resample.com). In each case, the bootstrap procedure resampled the larger of the two samples 1,000 times with the resampling size equivalent to the smaller of the two samples. Comparison was then made between the 95% confidence interval of the resampled means and the observed mean of the smaller sample.

Results for the entire fauna

Absolute sizes for all measured specimens in each formation are plotted in Figs. 2, 3. The Jupiter Formation had the most measured specimens (56) and identified specimens (244), whereas the Gun River Formation had the fewest (5) measured specimens and identified specimens (23). However, the percentage of measured to available specimens is relatively constant throughout the section at 25.1% (range for formation: 21.7–32.5%). The overall distribution of body sizes within a formation is also similar in all formations, with many smaller specimens and fewer larger specimens (although not evident in Fig. 2f because of the very small sample size, it also applies to the Gun River). The largest specimens from the Jupiter and Chicotte formations are significantly larger than from all other formations (Fig. 3, Table 1). Of formations older than the Jupiter, the Vauréal Formation has the largest specimens (Fig. 2).

These mean values are compared to the means of only measured specimens and means of species means in each formation (Table 2). There is variation in absolute values, but the same relative differences exist. There is an overall dominance of large specimens in the Chicotte Formation; and the Chicotte has the largest specimens of the Monobathrida, Dendrocrinida, Flexibilia, and Disparida (Table 3). The largest Cyathocrinida is in the Vauréal Formation, and the largest Diplobathrida is from the Ellis Bay Formation. The smallest Dendrocrinida and Flexibilia are from the Vauréal Formation, the smallest Cyathocrinida is from the Ellis Bay Formation, the smallest Diplobathrida is from the Becscie Formation, and the smallest Monobathrida and Disparid are from the Jupiter Formation.

The Mann–Whitney *U* test (Table 4) and bootstrapping (Fig. 4) indicate a statistically significant size decrease in crinoid calyx volume from the Vauréal to the Ellis Bay, which coincides with the end-Katian crinoid extinction identified by Peters and Ausich (2008). The Mann–Whitney *U* significance comparing Vauréal crinoid mean calyx volume to that of the Ellis Bay is $p = 0.035$ (Table 4). There is not a statistical difference between Ellis Bay and the Becscie ($p = 0.114$). Thereafter, a statistically significant difference exists in each additional step through the Anticosti Island stratigraphy, with a decrease between the Becscie and Gun River formations and increase between both the Gun River and Jupiter formations and the Jupiter and Chicotte formations (Table 4).

Evolutionary trends within clades

The trend of mean values through the section for major crinoid clades (subclasses or orders) is given in Fig. 5. Not all clades are represented in every formation, but the same general pattern exists for the entire fauna. Monobathrid specimens amenable to measurement do not occur in the Vauréal, but there is a decrease after the Ellis Bay and an increase thereafter (Fig. 5a, b). The trend for the disparids (from the Ellis Bay through the Jupiter formations) is basically the same as the monobathrids (Fig. 5f).

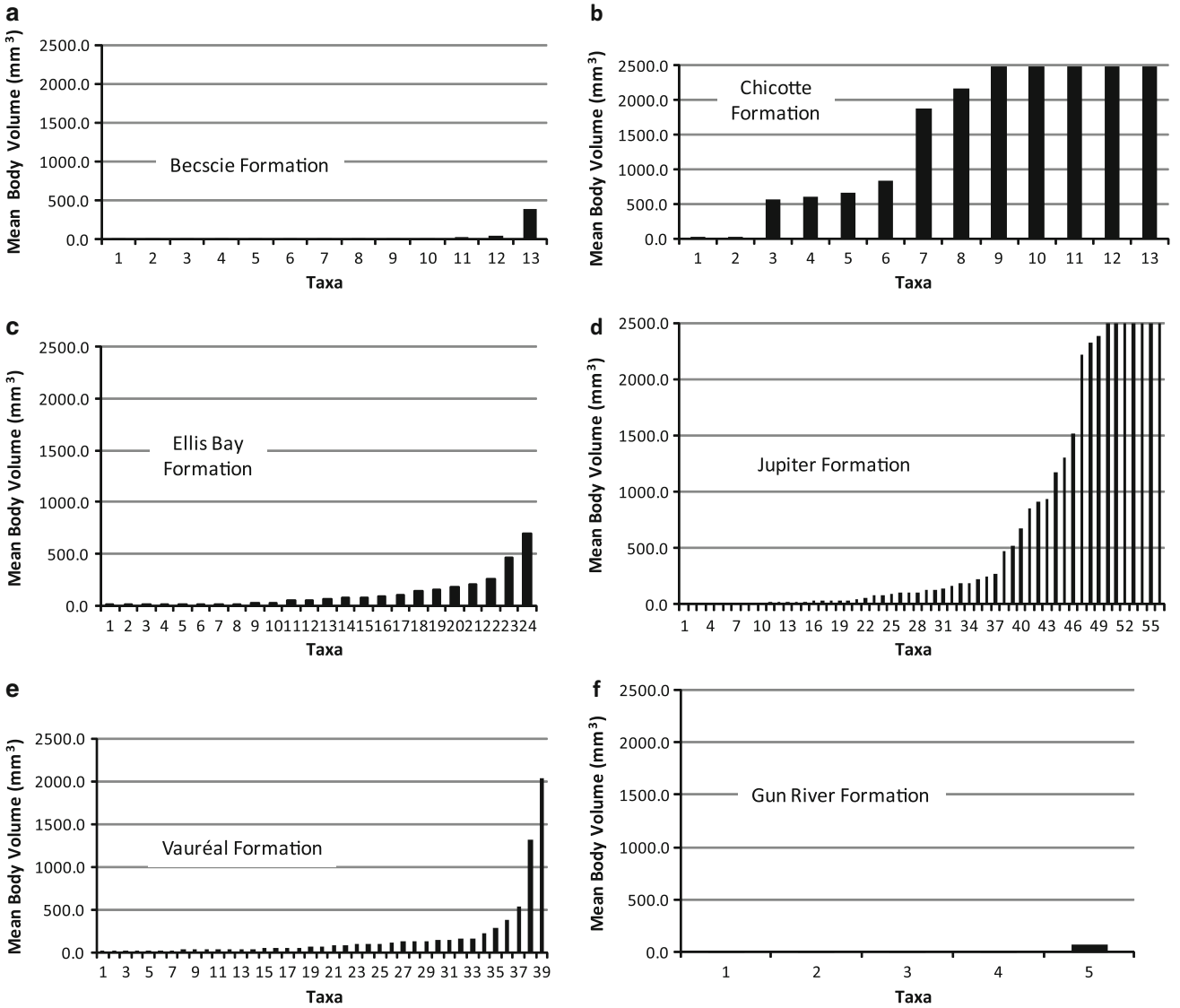

Fig. 2 Rank-order distribution of calyx volumes for each formation on Anticosti Island (note largest volumes truncated)

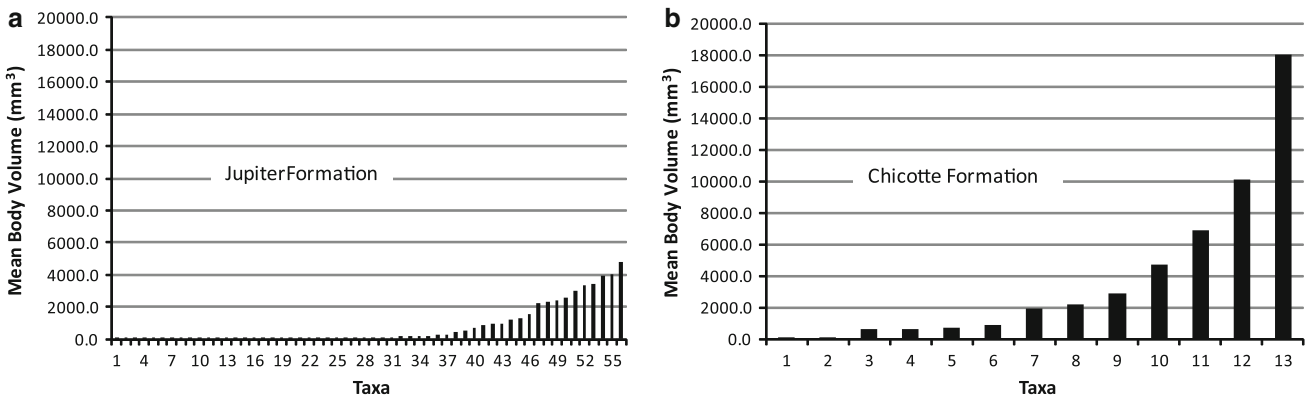

Fig. 3 Complete rank-order distribution of calyx volumes for the Jupiter and Chicotte formations

Table 1 Smallest and largest specimens in each formation

	Smallest species	Largest species
Chicotte Formation	2.3	12451.1
	Pisocrinus quinquelobus	*Abacocrinus latus*
	Disparida	Monobathrida
Jupiter Formation	1.2	4439.9
	Eomyelodactylus springeri	*Stiptocrinus hulveri*
	Disparida	Diplobathrida
Gun River Formation	1.8	74.1
	Eomyelodactylus donovani	*Stipatocrinus hulveri*
	Disparida	Monobathrida
Becscie Formation	2.6	398.2
	Dendrocrinus leptos	*Apoarchaeocrinus anticostiensis*
	Dendrocrinida	Diplobathrida
Ellis Bay Formation	2.8	695.5
	Dendrocrinus leptos	*Ursucrinus stellatus*
	Dendrocrinida	Diplobathrida
Vauréal Formation	0.8	2032.2
	Dendrocrinus minutus	*Carabocrinus boltoni*
	Dendrocrinida	Cyathocrinida

Measurements in mm^3

Table 2 Calyx volume means for each formation

Formation	All measured specimens	Species means for all measured specimens	All specimens with species means
Chicotte Formation	3792.7	2678.9	7267.5
Jupiter Formation	771.7	564.5	543.1
Gun River Formation	16.5	26.4	5.9
Becscie Formation	51.5	82.1	96.9
Ellis Bay Formation	112.6	160.8	122.4
Vauréal Formation	181.9	463.2	197.8

For "species means" the mean value of every species is averaged. For "all specimens," all collected specimens are included with the volume for each specimen the mean value for that species in that formation. Measurements in mm^3

The largest formation mean for diplobathrids is in the Ellis Bay Formation, indicating a large calyx volume increase from the Vauréal Formation before a drop to the Becscie. The importance of this different trend is unclear, because the Ellis Bay value is from a single specimen (*Ursucrinus stellatus* Ausich and Copper) (Fig. 5d). Other diplobathrids increase in size in the Jupiter Formation (Fig. 5c). Flexibles have a similar but less pronounced increase from the Vauréal to the Ellis Bay, then the flexibles' trend mirrors the general faunal trend thereafter. The entire pattern of dendrocrinids and cyathocrinids is consistent with the overall crinoid trend.

Table 3 The largest and smallest species in each major crinoid clade

	Smallest species	Largest species
Diplobathrida	8.0	4439.9
	Becsciecrinus adonis	*Bucucrinus saccus*
	Bescsie Formation	Jupiter Formation
Monobathrida	7.1	12451.1
	Jovacrinus jugum	*Abacocrinus latus*
	Jupiter Formation	Chicotte Formation
Dendrocrinida	0.8	2159.1
	Dendrocrinus minutus	*Myosocrinus chicottensis*
	Vauréal Formation	Chicotte Formation
Cyathocrinida	335.5	2032.20
	Euspirocrinus gagnoni	*Carabocrinus boltoni*
	Ellis Bay Formation	Vauréal Formation
Flexibilia	15.5	673.2
	Clidochirus vaurealensis	*Ladacrinus* sp.
	Vauréal Formation	Chicotte Formation
Disparida	1.2	576.9
	Eomyelodactylus springeri	*Corvucrinus schucherti*
	Jupiter Formation	Chicotte Formation

Measurements in mm^3

Table 4 Mann-Whitney *U* results for formational comparisons

	Chicotte	Jupiter	Gun River	Becscie	Ellis Bay	Vauréal
Chicotte	1					
Jupiter	<0.001	1				
Gun River	<0.001	<0.001	1			
Becscie	<0.001	0.02	<0.001	1		
Ellis Bay	<0.001	0.060	<0.001	0.114	1	
Vauréal	<0.001	0.063	<0.001	<0.001	0.035	X

A few crinoid families are represented in two or more formations, and these are illustrated in Fig. 6. Unfortunately, the data for each family are incomplete. However, given the available occurrences, families exhibit the basic pattern as for all crinoids. The lone exception is the change from the Vauréal to the Ellis Bay formations, where the Vauréal dendrocrinid is smaller than those of the Ellis Bay. Again, the Vauréal is only represented by a single, in this case, very small specimen, so its significance is unclear.

Disparids and diplobathids are clades characteristic of the early Paleozoic CEF; whereas monobathrids, cladids, and flexibles are characteristic of the middle Paleozoic

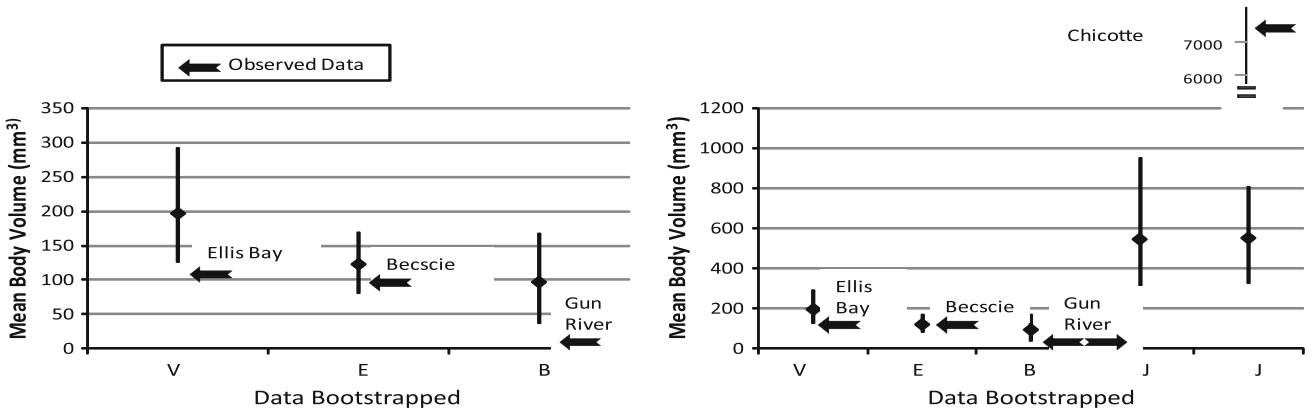

Fig. 4 Bootstrapping results comparing the 95% confidence intervals for a given formation to the mean of the observed calyx volumes from a subjacent or superjacent formation indicatged with an *arrow*. (*V* Vauréal Formation, *E* Ellis Bay Formation, *B* Becscie Formation, *J* Jupiter Formation)

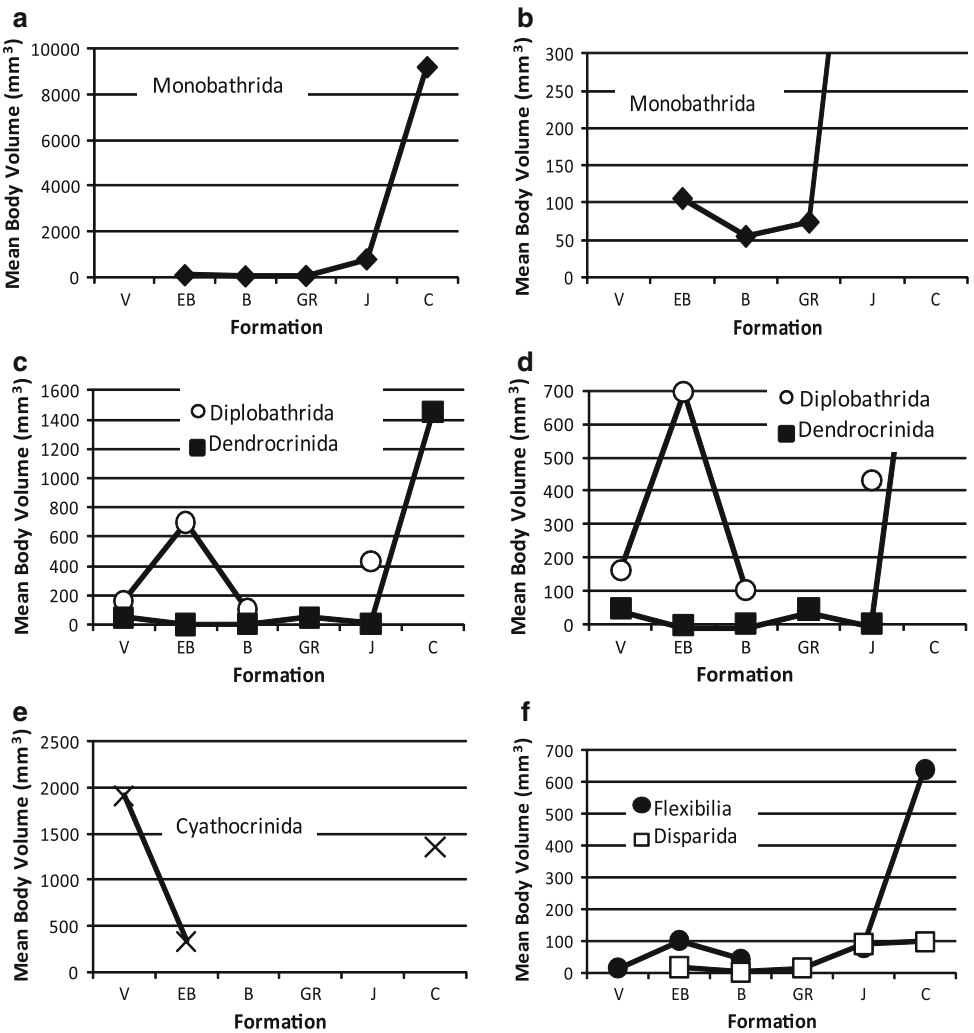

Fig. 5 Mean body volume in each formation for each major clade of Anticosti Island crinoid (*V* Vauréal Formation, *E* Ellis Bay Formation, *B* Becscie Formation, *GR* Gun River Formation, *J* Jupiter Formation, *C* Chicotte Formation)

CEF. There is no distinction among size change patterns of clades from the contrasting CEFs across the Ordovician–Silurian boundary. Further, all clades rebound in body size by at least the Telychian Chicotte Formation.

Discussion

Unlike later in their history, crinoid macroevolutionary dynamics were directly affected by global extinction

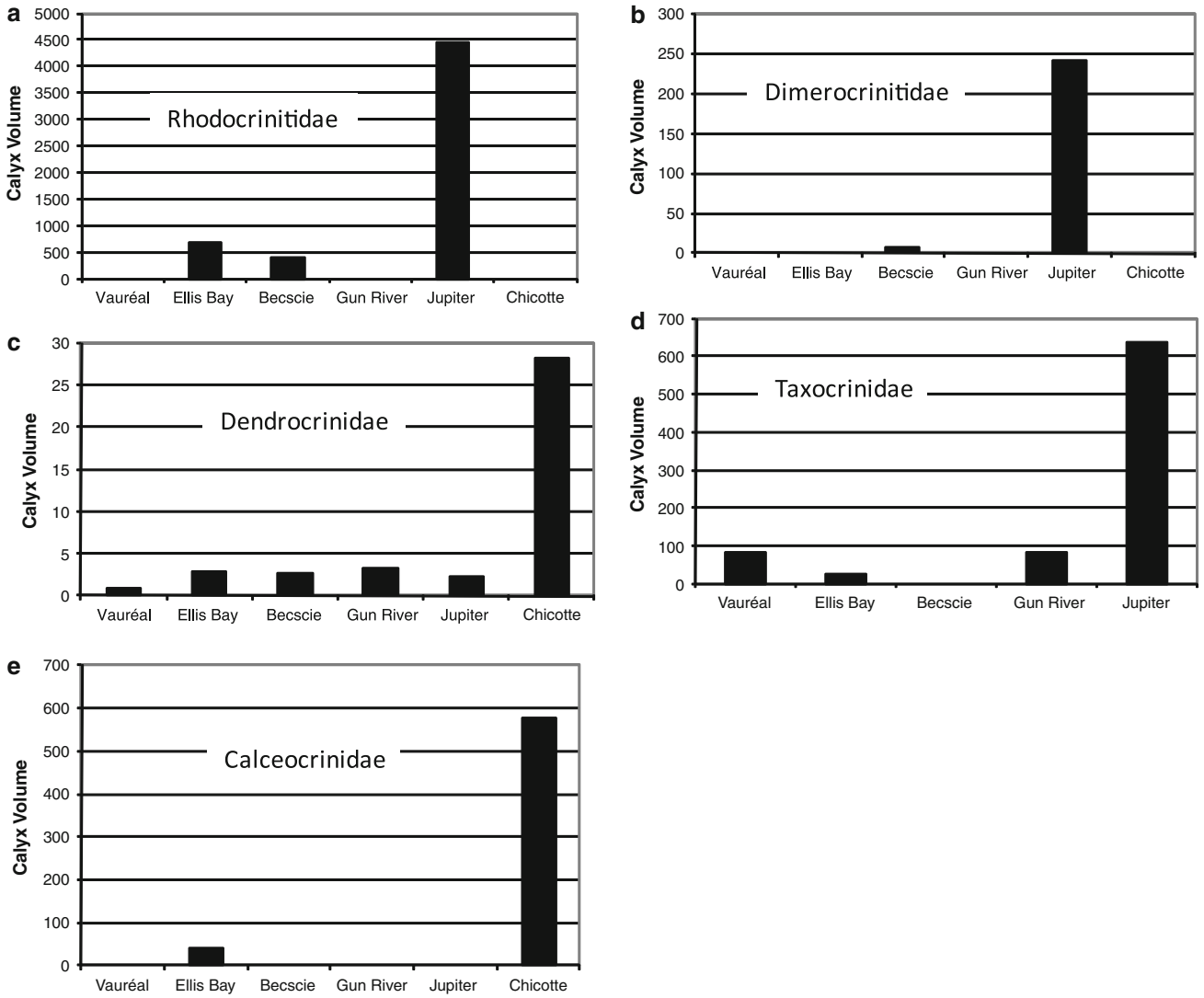

Fig. 6 Mean calyx volume in each formation for each family that has multiple representation in formations through the Anticosti stratigraphy

pressures during the end-Ordovician interval (compare Ausich et al. 1994 and Peters and Ausich 2008). The end-Ordovician biotic crisis induced the Lilliput Effect among crinoids, as evidenced by significant crinoid size reduction through the end-Ordovician extinction interval on Anticosti Island.

The stage-level time slices through the Anticosti Island succession range from approximately 1.5–4.7 Ma (Ogg et al. 2008); therefore, the data analyzed here can only be interpreted from an evolutionary time perspective. As presently understood, no species and only three genera cross the Katian–Hirnantian global extinction interval on Anticosti Island, and only one species and four genera range through the Hirnantian to the Rhuddanian (Ordovician–Silurian boundary on Anticosti Island) (Ausich and Copper 2010). 18% (2 of 11) of the Hirnantian and 43% (3 of 7) of the Becscie Formation crinoid genera on Anticosti Island are new. Consequently, Anticosti Island crinoids through the end-Ordovician biotic crisis correspond to the miniaturization mode of the Lilliput Effect, which resulted from the evolution of new, smaller taxa during the recovery phase of mass extinction.

A variety of facies are preserved on Anticosti Island. Most formations contain a diversity of facies from deep to shallow environments (Copper and Long 1998, among many others). It is possible that the Lilliput Effect size-reduction in this boundary-crossing fauna may indicate convergent adaptations in separate lineages to paleoenvironmental conditions. The smallest specimens occur in the Ellis Bay, Becscie, and Gun River formations. The deep-water Gun River Formation almost exclusively contains very small specimens. However, the Ellis Bay and Becscie formations are represented by both deep- and shallow-water facies, as are other formations with crinoids. The Vauréal to

Ellis Bay boundary and the Ordovician–Silurian boundary are bounded by strata that represent very shallow-water facies in the Laframboise Member of the Ellis Bay Formation and the Fox Point Member of the Becscie Formation. Another pertinent comparison is among reefal facies. Very small crinoids are associated with reefs in the Laframboise Member of the Ellis Bay Formation (mean = 99.1 mm^3; SD = 94.8), immediately below the Ordovician–Silurian boundary. In contrast, crinoids associated with reefs during the Silurian (East Point Member of the Jupiter Formation and the Chicotte Formation) are among the largest crinoids on the island. The Silurian reef-associated faunas had mean volumes of 1,872.2 mm^3 (SD = 760.1) for the East Point member; and Chicotte crinoids are even larger, although it is difficult in all cases to separate non-reef from reef-associated Chicotte specimens. Therefore, water depth and depositional facies cannot be argued as the primary factor controlling the body size of these animals. Rather, factors other than paleoenvironmental and facies conditions, such as a deteriorating climate and community dynamics must have exerted a more direct control on crinoid success and maximum body sizes. This trend counters that identified for the Ordovician radiation when body size increased among trilobites and brachiopods (Finnegan and Droser 2009).

Getting small

The estimated body sizes discussed here are the volumes of the crinoid calyx, i.e., from the point where arms become free to the top of the column. This volume is directly correlated with the mass of calcite secreted in the body wall and the volume of viscera (digestive system, reproductive system, and other coelomic tissues.) Thus, the calyx volume reflects the metabolic costs of body building. If one infers a correlation in viscera volume to the volume of gonads, calyx size may also be correlated to fecundity. Overall body size also affects an organisms' "niche placement." Although there is not a direct correlation of calyx or crown size to column height, it is reasonable to assume that a crinoid with a one or more order of magnitude smaller body would simply be a smaller crinoid with a shorter column, thus closer to the sea floor in lower tiers (Ausich 1980; Ausich and Bottjer 1982; Bottjer and Ausich 1987). Brower (2006) demonstrated that calyx size is positively correlated to the length of the ambulacral tracts, thus the area of the filtration fan would also be smaller.

Thus, a smaller crinoid would presumably have lower fecundity and a diminished feeding capacity relative to its larger ancestor. These "disadvantages" may reflect adaptations to less-stable ecological conditions. Lower fecundity of a smaller crinoid could be offset by smaller crinoids reaching sexual maturity more rapidly. The diminished feeding capacity of a smaller filtration fan would be offset by a smaller crinoid requiring less caloric intake for growth and maintenance. Further, crinoids are segregated into niches based on the size of food particles they capture, which is primarily controlled by clade-specific parameters.

As discussed above, body size contrasts can commonly be explained as alternative life strategies. Understanding the reasons faunas experience the Lilliput Effect is not straightforward; and, of course, more than one cause may be responsible. In the case of Ordovician to Silurian crinoids, the cause(s) apparently left a record in data preserved at an evolutionary time resolution. Of the processes discussed above, a change in salinity, oxygen levels, and loss of symbionts can be eliminated because crinoids lack any photosynthetic symbionts and the Anticosti Island strata were deposited in a normal, open marine setting throughout the interval in question. Furthermore, based on available data (Ausich in prep.), there is no indication that the Hirnantian and Rhuddanian faunas were derived largely from a higher latitude, cooler-water Katian fauna, such as among brachiopods (Sheehan 1973; Rong et al. 2006).

None of the other potential causes can be eliminated; and in fact, they could all be interrelated. These include biotic collapse in primary productivity, general biotic stress, temperature changes, and the Island Rule. There is not a doubt that the expansive shallow-water habitats of Ordovician epicontinental seas were largely eliminated globally. Anticosti Island was positioned in a foreland basin along the margin of Laurentia. The substantially smaller potential habitat was at least partially responsible for the significant biodiversity decline and could certainly have been a factor controlling overall body size.

It is also reasonable to assume a decrease in primary productivity in the oceans and an increase in general biotic stress would have accompanied the end-Ordovician climatic deterioration and the nearly complete loss of shallow-water habitats. In order to survive stressed conditions during this the biotic crisis, Ellis Bay and Becscie crinoids may have accelerated the onset of sexual maturity, thus reaching reproductive age earlier at smaller body sizes. This reduction in generation time and increase in genetic diversity per unit time may have provided opportunities for evolutionary novelty that led to new taxa. It is also possible that the success of crinoids through this crisis was dependent on evolutionary novelty, which eventually resulted in the radiation of the middle Paleozoic CEF that was firmly established by the late Llandovery (Ausich 1984). The asymmetrical macroevolutionary pattern of size change among crinoids is consistent with the pattern for taxic data (Peters and Ausich 2008). These latter authors compared crinoid turnover rates through this stratigraphic interval to sediment package turnover rates. The two parameters were correlated through the end-Katian

extinction but were not correlated during the recovery. Peters and Ausich (2008) argued that the contraction of epicontinental seas and all of the associated environmental stresses (common cause hypothesis of Peters 2005) were responsible for the extinctions. However, the faunal recovery was delayed, perhaps because various biotic factors and evolutionary processes took more time for recovery. Similarly, the body volume data indicate that the end-Katian extinction occurred very rapidly (given the temporal resolution). The recovery occurred during an interval of cyclic climatic change, and it took as many as 7 Ma. This is another study that may have a profound impact on our view of the present-day biotic crisis, because rapid decreases in biodiversity and morphological disparity may take millions of years to recover, based on the results presented here.

Conclusions

1. On Anticosti Island, the Ellis Bay Formation contains evidence of a distinct crinoid fauna that has a statistically significant smaller body size than previous crinoid faunas. Crinoid calyx volume was larger again by the late Aeronian and Telychian.
2. This interval of size decrease coincided with a global mass extinction of crinoids
3. Reduced body size co-occurs with the environmental stresses induced by a rapid, severe reduction of shallow habitats and climate cooling, resulting from the end-Ordovician glacial epoch.
4. Elements of the middle Paleozoic CEF were not established by a more successful adaptation to diminutive body size, although a more rapid recovery of size may have allowed cladids, monobathrids and flexibles to seize on large-bodied niches formerly occupied by the morphologically diverse Early Paleozoic crinoid fauna.
5. Along with work on Early Silurian corals, this study marks the oldest reported incidence of the Lilliput Effect, and further establishes the Lilliput Effect as a significant evolutionary trend coincident with the first of the "Big Five" mass-extinction events.

Acknowledgments This work was supported by National Geographic Society grant 6789-00 and NSF grant EAR-0205968 to WIA. Careful reviews by George D. Sevastopulo and Gary D. Webster improved this manuscript.

References

Ausich, W. I. (1980). A model for niche differentiation in lower Mississippian crinoid communities. *Journal of Paleontology, 54*, 273–288.

Ausich, W. I. (1984). Calceocrinids from the Early Silurian (Llandoverian) Brassfield Formation of southwestern Ohio. *Journal of Paleontology, 58*, 1167–1185.

Ausich, W. I., & Bottjer, D. J. (1982). Tiering in suspension-feeding communities on soft substrata throughout the Phanerozoic. *Science, 216*(4542), 173–174.

Ausich, W. I., Brett, C. E., Hess H., & Simms, M. J. (1999). Crinoid form and function. In H. Hess, W. I. Ausich, C. E. Brett & M. J. Simms (Eds.) *Fossil Crinoids* (pp 3–30). Cambridge: Cambridge University Press

Ausich, W. I., & Copper, P. (2010). Anticosti Island Crinoid Monograph. *Palaeontographica Canadiana*, *29*, 157

Ausich, W. I., Kammer, T. W., & Baumiller, T. K. (1994). Demise of the middle Paleozoic crinoid fauna: a single extinction event or rapid faunal turnover? *Paleobiology, 20*, 345–361.

Barnes, C. R., & Bergström, S. M. (1988). Conodont biostratigraphy of the uppermost Ordovician and lowermost Silurian. *British Museum of Natural History (Geology) Bulletin, 84*, 325–343.

Baumiller, T. K. (1993). Survivorship analysis of Paleozoic Crinoidea: effect of filter morphology on evolutionary rates. *Paleobiology, 19*, 304–321.

Bergmann, C. (1847). Über die Verhältnisse der wärmeökonomie der Tiere zu ihrer Grösse. *Göttinger Studien*, *3*, 595–708.

Berry, W. B. N., & Boucot, A. J. (1973). Glacioeustatic control of Late Ordovician–Early Silurian platform sedimentation and faunal change. *Bulletin of Geological Society of America*, *84*, 275–284.

Bottjer, D. J., & Ausich, W. I. (1987). Phanerozoic development of tiering in soft substrata suspension-feeding communities. *Paleobiology, 12*, 400–420.

Brenchley, P. J. (1989). The Late Ordovician Extinction. In S. K. Donovan (Ed.), *Mass extinctions: processes and evidence* (pp. 104–132). New York: Columbia University Press.

Brenchley, P. J., Carden, G. A. F., Hints, L., Kaljo, D., Marshall, J. D., Martma, T., et al. (2003). High-resolution stable isotope stratigraphy of upper Ordovician sequences: constraints on the timing of bioevents and environmental changes associated with mass extinction and glaciation. *Geological Society of America Bulletin, 115*, 89–104.

Brenchley, P. J., Marshall, J. D., Carden, G. A. F., Robertson, D. B. R., Long, D. G. F., Meidla, T., et al. (1994). Bathymetric and isotopic evidence for a short-lived Late Ordovician glaciation in a greenhouse period. *Geology, 22*, 295–298.

Brower, J. C. (1978). Camerates. In R. C. Moore & C. Teichert (Eds.), *Treatise on invertebrate paleontology, Part T Echinodermata 2 (1)* (pp. T244–T263). Lawrence, Kansas: Geological Society of America and University of Kansas Press.

Brower, J. C. (2006). Ontogeny of the food-gathering system in Ordovician crinoids. *Journal of Paleontology*, *80*, 430–446.

Chen, X., Melchin, M. J., Fan, J. & Mitchell, C. E. (2003). Ashgillian graptolite fauna of the Yangtze region and the biogeographical distribution of diversity in the latest Ordovician. *Bulletin de la Societe Geologique de France*, *174*, 141–148.

Copper, P. (1986). Fransian/Famennian mass extinction and cold-water oceans. *Geology, 14*, 835–839.

Copper, P. (2001). Reefs during multiple crises towards the Ordovician–Silurian boundary: Anticosti Island, eastern Canada, and worldwide. *Canadian Journal of Earth Sciences, 38*, 153–171.

Copper, P., & Long, D. G. F. (1989). Stratigraphic revisions for a key Ordovician–Silurian boundary section, Anticosti Island, Canada. *Newsletters on Stratigraphy, 21*, 59–73.

Copper, P., & Long, D. G. F. (1998). Field guide to carbonates and reefs of Anticosti Island, Québec. In A. Desrochers, P. Copper & D. Long (Eds.), *Paleontology stratigraphy and sedimentology of lower to middle Paleozoic rocks of the Anticosti Basin: National*

Park of Mingon Islands and Anticosti Island (pp. 1–97). Geological Association of Canada B Mineralogical Association of Canada, Joint Meeting, Quebec, Field Trip B8 Guidebook.

Desrochers, A., Farley, C., Achab, A., Asselin, A., & Riva, J. F. (2010). A far-field record of the end Ordovician glaciation: the Ellis Bay Formation, Anticosti Island, Eastern Canada. *Palaeogeography, Palaeoclimatology, Palaeoecology, 296*, 248–263.

Donovan, S. K. (1989). The significance of the British Ordovician crinoid fauna. *Modern Geology, 13*, 243–255.

Donovan, S. K. (1994). The Late Ordovician extinctions of crinoids in Britain. *National Geographic Research and Exploration, 10*, 72–79.

Eckert, J. D. (1988). Late Ordovician extinction of North American and British crinoids. *Lethaia, 21*, 147–167.

Finnegan, S., & Droser, M. L. (2009). Body size, energetics, and the Ordovician restructuring of marine ecosystems. *Paleobiology, 34*, 342–359.

Finney, S. C., Berry, W. B. N., Cooper, J. D., Ripperdan, R. L., Sweet, W. C., Jacobson, S. R., et al. (1999). Late Ordovician mass extinction: a new perspective from stratigraphic sections in central Nevada. *Geology, 27*, 215–218.

Ghienne, J. (2003). Late Ordovician sedimentary environments, glacial cycles, and post-glacial transgression in the Taoudeni Basin, West Africa. *Palaeogeography, Palaeoclimatology, Palaeoecology, 189*, 117–145.

Girard, C., & Renaud, S. (1996). Size variations in conodonts in response to the upper Kellwasser crisis (upper Devonian of the Montagne Noire, France). *Comptes Rendus de l'Academie des Sciences Serie IIa, 323*, 435–442.

Grahn, Y., & Caputo, M. V. (1992). Early Silurian glaciations in Brazil. *Palaeogeography, Palaeoclimatology, and Palaeoecology, 99*, 9–15.

Grahn, Y., & Caputo, M. V. (1994). Late Ordovician evolution of the intracratonic basins in north-west Gondwana. *Geologische Rundschau, 84*, 665–668.

Hallam, A. & Wignall, P.B. (1997). Latest Ordovician extinctions: one disaster after another. In A. Hallam & P. B. Wignall (Eds.), *Mass extinctions and their aftermath* (pp. 39–57). New York: Oxford University Press.

Hammer, Ø., Harper, D. A. T. & Ryan, P. D. (2001). PAST: paleontological statistics software package for education and data analysis. *Palaeontologia Electronica*, *4*(1), 1–9. http://palaeo-electronica.org/2001_1/past/issue1_01.htm.

Harper, D. A. T., & Rong, J. (1995). Patterns of change in the brachiopod faunas through the Ordovician–Silurian interface. *Modern Geology, 20*, 83–100.

Harries, P. J., & Knor, P. O. (2009). What does the 'Lilliput Effect' mean? *Palaeogeography, Palaeoclimatology, Palaeoecology, 284*, 4–10.

Herrmann, A. D., Haupt, B. J., Patzkowsky, M. E., Seidov, D., & Slingerland, R. L. (2004b). Response of Late Ordovician paleoceanography to changes in sea level, continental drift, and atmospheric pCO_2: potential causes for long-term cooling and glaciation. *Palaeogeography, Palaeoclimatology, Palaeoecology, 210*, 385–401.

Herrmann, A. D., Patzkowsky, M. E., & Pollard, D. (2004a). The impact of paleogeography pCO_2, poleward ocean heat transport and sea level change on global cooling during the Late Ordovician. *Palaeogeography, Palaeoclimatology, Palaeoecology, 206*, 59–74.

Hone, D. W. E., & Benton, M. J. (2005). The evolution of large size: how does Cope's Rule work? *Trends in Ecology and Evolution, 20*, 4–7.

Hone, D. W. E., & Benton, M. J. (2007). Cope's Rule in the Pterosauria and differing perceptions of Cope's Rule at differing taxonomic levels. *Journal of Evolutionary Biology, 20*, 1164–1170.

Hone, D. W. E., Keesey, T. M., Pisani, D., & Purvis, A. (2005). Macroevolutionary trends in Dinosauria: Cope's Rule. *Journal of Evolutionary Biology, 18*, 587–595.

Kaljo, D. (1996). Diachronous recovery patterns in Early Silurian corals, graptolites, and acritarchs. In M. B. Hart (Ed.), *Biotic recovery after mass extinction events*. Geological Society Special Publication 102, 127–133.

Kaljo, D., Hints, L., Männik, P., & Nolvak, J. (2008). The succession of Hirnantian events based on data from Baltica: brachiopods, chitinozoans, conodonts, and carbon isotopes. *Estonian Journal of Earth Sciences, 57*, 197–218.

Kump, L. R., Arthur, M. A., Patzkowsky, M. E., Gibbs, M. T., Pinkus, D. S., & Sheehan, P. M. (1999). A weathering hypothesis for glaciation at high atmospheric pCO_2 during the Late Ordovician. *Palaeogeography, Palaeoclimatology, Palaeoecology, 152*, 173–187.

Lefebvre, V., Servais, T., François, L., & Averbuch, O. (2010). Did a Katian large igneous province trigger the Late Ordovician glaciation? A hypothesis tested with a carbon cycle model. *Paleogeography, Palaeoclimatology, Palaeoecology, 296*, 310–319.

Lockwood, R. (2005). Body size, extinction events, and early Cenozoic record of veneroid bivalves; a new role for recoveries? *Paleobiology, 31*, 578–590.

Long, D. G. F. (2007). Tempestite frequency curves: a key to Late Ordovician and Early Silurian subsidence, sea level change, and orbital forcing in the Anticosti foreland basin, Quebec, Canada. *NRC Canada, 44*, 413–431.

Long, D. G. F., & Copper, P. (1987). Stratigraphy of the Upper Ordovician Vauréal and Ellis Bay Formations, eastern Anticosti Island. *Canadian Journal of Earth Sciences, 24*, 1807–1820.

McKerrow, W. S. (1979). Ordovician and Silurian changes in sea level. *Journal of the Geological Society, 136*, 137–146.

Meire, S., & Dayan, T. (2003). On the validity of Bergmann's rule. *Journal of Biogeography, 30*, 331–351.

Melott, A. L., & Thomas, B. C. (2009). Late Ordovician geographic patterns of extinction compared with simulations of astrophysical ionizing radiation damage. *Paleobiology, 35*, 311–320.

Ogg, J. G., Ogg, G., & Gradstein, F. M. (2008). *The Concise Geologic Time Scale* (p. 177). Cambridge: Cambridge University Press

Peters, S. E. (2005). Geological constraints on the macroevolutionary history of marine animals. *Proceedings of the National Academy of Sciences, USA, 102*, 12326–12331.

Peters, S. E., & Ausich, W. I. (2008). A sampling-adjusted macroevolutionary history for Ordovician-Early Silurian crinoids. *Paleobiology, 34*, 104–116.

Rong, J.-Y., Boucot, A. J., Harper, D. A. T., Zahn, R.-B., & Newman, R. B. (2006). Global analysis of brachiopod faunas through the Ordovician and Silurian transition: reducing the role of the Lazarus effect. *Canadian Journal of Earth Sciences, 43*, 23–39.

Schmidt, D. N., Thierstein, H. R., & Bollman, J. (2004). The evolutionary history of size variation of planktic foraminiferal assemblages in the Cenozoic. *Palaeogeography, Palaeoclimatology, Palaeoecology, 212*, 159–180.

Sepkoski, J. J., Jr. (1981). A factor analytic description of the marine fossil record. *Paleobiology, 7*, 36–53.

Sheehan, P. M. (1973). The relation of Late Ordovician to Ordovician–Silurian changeover in North America brachiopod faunas. *Lethaia, 6*, 147–154.

Sheehan, P. M. (2001). The Late Ordovician mass extinction. *Annual Review of Earth and Planetary Sciences, 29*, 331–364.

Stanley, S. M. (1973). An explanation for Cope's rule. *Evolution, 27*, 1–26.

Sutcliffe, O. E., Dowdeswell, J. A., Whittington, R. J., Theron, J. N., & Craig, J. (2000). Calibrating the Late Ordovician glaciation and mass extinction by the eccentricity cycles of Earth's orbit. *Geology, 28*, 967–970.

Twitchett, R. J. (2006). The palaeoclimatology, palaeoecology and paleoenvironmental analysis of mass extinction events. *Palaeogeography, Palaeoclimatology, Palaeoecology, 232*, 190–213.

Twitchett, R. J. (2007). The Lilliput effect in the aftermath of the end-Permian extinction event. *Palaeogeography, Palaeoclimatology, Palaeoecology, 252*, 132–144.

Ubaghs G. (1978). Skeletal morphology of fossil crinoids. In R. C. Moore & C. Teichert (Eds.), *Treatise on invertebrate paleontology, Part T Echinodermata 2 (1)* (pp. T58–T216). Lawrence, Kansas: Geological Society of America and University of Kansas Press.

Urbanek, A. (1993). Biotic Crises in the history of Upper Silurian graptoloids: a paleobiological model. *Historical Biology, 7*, 29–50.

Van Valen, L. (1973). Pattern and the balance of nature. *Evolutionary Theory, 1*, 31–49.

Wade, B. S., & Olsson, R. K. (2009). Investigation of pre-extinction dwarfing in Cenozoic planktonic foraminifera. *Palaeogeography, Palaeoclimatology, Palaeoecology, 284*, 39–46.

Wade, B. S., & Peterson, P. N. (2008). Planktonic foraminiferal turnover, diversity fluctuations and geochemical signals across the Eocene/Oligocene boundary in Tanzania. *Marine Micropaleontology, 68*, 244–255.

Wade, B. S., & Twitchett, R. J. (2009). Extinction, dwarfing, and the Lilliput effect. *Palaeogeography, Palaeoclimatology, Palaeoecology, 284*, 1–3.

Waldron, J. W. F., Anderson, S. D., Carwood, P. A., Goodwin, L. B., Hall, J., Jamieson, R. A., et al. (1998). Evolution of the Appalachian Laurentian margin: Lithoprobe results in western Newfoundland. *Canadian Journal of Earth Sciences, 35*, 1271–1287.

Weihong, H., Shi, G. R., Feng, Q., Campi, M. J., Gu, S., Bu, J., et al. (2006). Brachiopod miniaturization and its possible causes during the Permian-Triassic crisis in deep water environments, South China. *Palaeogeography, Palaeoclimatology, Palaeoecology, 252*, 145–163.

Young, S. A., Saltzman, M. R., Derochers, A., Ausich, W. I., & Kaljo, D. (2010). Did changes in atmospheric CO_2 coincide with Late Ordovician glacial-interglacial cycles? *Paleogeography, Palaeoclimatology, Palaeoecology, 296*, 376–388.